

Article

Microstructure and Mechanical Properties of the Dactylopodites of the Chinese Mitten Crab (*Eriocheir sinensis*)

Ying Wang ¹, Xiujuan Li ^{1,*} , Jianqiao Li ¹ and Feng Qiu ² 

¹ Key Laboratory of Bionic Engineering, Ministry of Education, Jilin University, Changchun 130025, China; shadowying7@163.com (Y.W.); jqli@jlu.edu.cn (J.L.)

² Key Laboratory of Automobile Materials, Ministry of Education, Department of Materials Science and Engineering, Jilin University, Changchun 130025, China; qiufeng@jlu.edu.cn

* Correspondence: xiujuanli@jlu.edu.cn; Tel.: +86-431-8509-5760

Received: 1 April 2018; Accepted: 21 April 2018; Published: 26 April 2018



Abstract: The dactylopodites of the Chinese mitten crab (*Eriocheir sinensis*) have evolved extraordinary resistance to wear and impact loading after direct contact with rough surfaces or clashing with hard materials. In this study, the microstructure, components, and mechanical properties of the dactylopodites of the Chinese mitten crab were investigated. Images from a scanning electron microscope show that the dactylopodites' exoskeleton was multilayered, with an epicuticle, exocuticle, and endocuticle. Cross sections and longitudinal sections of the endocuticle revealed a Bouligand structure, which contributes to the dactylopodites' mechanical properties. The main organic constituents of the exoskeleton were chitin and protein, and the major inorganic compound was CaCO₃, crystallized as calcite. Dry and wet dactylopodites were brittle and ductile, respectively, characteristics that are closely related to their mechanical structure and composition. The findings of this study can be a reference for the bionic design of strong and durable structural materials.

Keywords: dactylopodite; microstructure; composition; mechanical properties

1. Introduction

After hundreds of millions of years of evolution, the functional properties of parts of organisms tend to have optimal structural and material characteristics, as well as excellent adaptability and longevity [1,2]. The strong exoskeletons of decapod crustaceans such as crabs and lobsters are an adaptation to harsh environments [3] and play important roles in supporting the body, resisting impacts from external forces, providing protection from external erosion, predators, and disease, and preventing the evaporation of water [4–6].

The Chinese mitten crab (*Eriocheir sinensis*) is a widespread freshwater crustacean. It has an impressive ability to move on hard and deformable terrain, such as mire. Due to their unique strong shell and means of locomotion, Chinese mitten crabs are able to adapt to a variety of complex terrains, a characteristic that has attracted widespread attention from researchers [7–10]. Most studies of crustaceans' hard shells have focused on pincers and other parts [3,8], whereas studies of pereopods have focused mostly on gait, kinematics, and energy conversion [11,12]. However, in adaptation to complex terrains, in addition to the Chinese mitten crabs' means of locomotion, their dactylopodites, which come into contact with the terrain during movement, also play an important role [13]. As the end parts of the pereopods, dactylopodites are in direct contact with rough ground and clash with hard materials such as gravel. They possess excellent mechanical properties and unique biological characteristics, such as shape, structure, and composition. Studies on the dactylopodites of the Chinese mitten crab are scarce.

This paper presents an analysis of the shape, structure, components, and mechanical properties of the dactylopodites of Chinese mitten crabs, helping us to further understand the excellent adaptability and athletic ability of these crustaceans. The research will provide new bionic design methods for strong and durable structural materials, which would be applied to the development and preparation of walking mechanism design with optimal performance, optimization of environmental adaptation, and minimum energy consumption on soft road terrain.

2. Experimental Methods

2.1. Preparation of Dactylopodite Samples from Chinese Mitten Crabs

Chinese mitten crabs (Figure 1) were purchased from an aquatic products market in Changchun, China. Seven crabs were selected, of which four were male (two were larger, two were smaller) and three were female. Table 1 shows the crabs' shell sizes (length \times width) and their weights. Studies have shown that the second and third pairs of paraeiopods are important for movement; therefore, the second and third paraeiopods were selected as the subjects of study. The dactylopodites were removed from the propodite–dactylopodite joints (as shown in Figure 1) for experimental use.

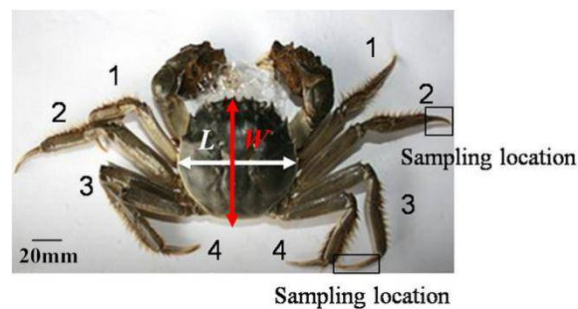


Figure 1. Chinese mitten crab.

Table 1. Parameters of Chinese mitten crab specimens.

Specimen	Dimension		Weight (g)
	Length (mm)	Width (mm)	
1 (male)	71.21	64.03	167
2 (male)	68.42	62.38	174
3 (male)	57.46	52.73	92
4 (male)	55.74	51.61	81
5 (female)	54.81	51.32	77
6 (female)	56.12	51.18	75
7 (female)	51.50	49.22	63
Mean \pm SD	59.32 \pm 7.44	54.64 \pm 5.96	104.14 \pm 46.18

2.2. Biological Characteristics of Chinese Mitten Crabs

2.2.1. Microstructure of the Dactylopodites

To obtain high-quality microstructure images, the surface of the specimens to be observed should be flat, and the structure should be clear. When samples were taken, a Cartesian coordinate grid was established with the dactylopodite as the origin (Figure 2). The dactylopodites were divided into five segments along the x -axis with a surgical blade, and the film and muscles inside were removed. The segments were marked 1, 2, 3, 4, and 5 in order of decreasing cross-sectional diameter, left to dry naturally, and then sprayed gold. The structures of the cross sections were observed with a scanning

electron microscope (SEM) (Zeiss EVO 18, Cambridge, UK). When observing the longitudinal section structure, the segments were cut along the axis of the dactylopodite.

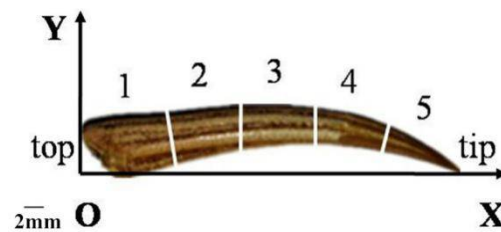


Figure 2. Coordinate grid with Chinese mitten crab dactylopodites.

2.2.2. Composition of the Dactylopodites

X-ray diffraction (XRD) (Model D/Max 2500PC Rigaku, Tokyo, Japan) and Fourier transform infrared (FTIR) analyses were conducted to identify the components of the Chinese mitten crab dactylopodites.

Samples for XRD were prepared by breaking fragments from the dactylopodites, removing the muscle tissue, drying the fragments naturally, and crushing and grinding them into a powder in a mortar until the particle size was about 45 μm . The detection apparatus was an X-ray diffractometer with Cu-K α radiation ($\lambda = 1.540598 \text{ \AA}$).

For the FTIR analysis, the dried dactylopodites were crushed and ground into a fine powder and then scattered evenly on a glass slide and compacted to form a sample. A Shimadzu Fnr-8400S (Shimadzu Corporation, Kyoto, Japan) was used to detect the components. The frequency range of the experiment was 400 to 4000 cm^{-1} .

2.3. Three-Point Bending Tests

The second and third pairs of dactylopodites were selected for three-point bending tests and divided into dry and wet samples. To prepare the dry samples, the dactylopodites were placed in separate aluminum boxes, and the weights of all the dactyli and boxes were measured with an electronic balance (JJ323BC, G & G, Suzhou, China). The samples were then put into drying boxes at 80 $^{\circ}\text{C}$ and dried for 4 h. The weights were then recorded, and the samples were returned to the drying boxes for another hour. If no change was recorded, drying was stopped; otherwise, drying continued until the weight did not change.

To prepare the wet samples, the segmented dactylopodites were soaked in water about 1 h. To prevent moisture loss and to prevent the samples becoming soft after soaking, which would affect their mechanical properties, the tests were completed within 4 h.

Considering the actual working conditions of the specimen, the test positions were selected and marked as 2/5 from the top of the dactylopodite (Figure 2). The maximum diameter d and length l at each marked place on the specimens were measured with a Vernier caliper. Three-point bending experiments were carried out using a small in situ tension tester (Changchun Mechanical Science Institute, maximum load 50 N, 220 V, 50 Hz). At least five samples were selected for each test. The test span was 15 mm, and the pressure head moved at 3 mm/min. Each sample was fixed on the holders, then a pressure head was moved towards it driven by a motor. When the indenter was exposed to the sample, the computer began to automatically record the load on the sample and the displacement data. The tests were stopped when the samples reached the yield point or broke.

3. Results and Discussion

3.1. Structural Property

3.1.1. Microstructure of Cross Section of a Dactylopodite

A layered structure is characteristic of the exoskeletons of crustaceans [14]. Numerous studies have shown that most exoskeletons include an epicuticle, an exocuticle, and an endocuticle [9,10,15]. The SEM results showed that a cross section of a Chinese mitten crab dactylopodite contains three layers, as shown in Figure 3. The epicuticle, which is a thin layer of wax on the outer surface of the dactylopodite, is easy to peel off in the dry state. The middle layer is the exocuticle, and the inner layer is the endocuticle.

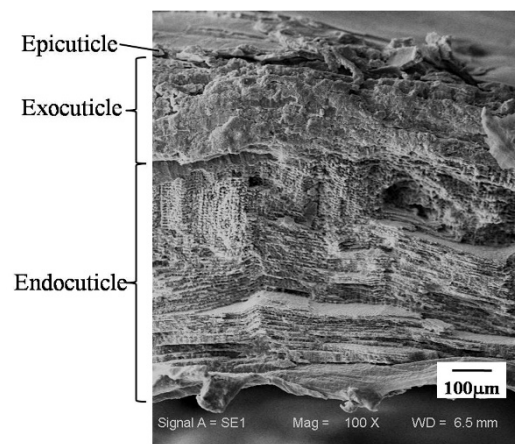


Figure 3. Multilayered structure of Chinese mitten crab dactylopodite.

Figure 4 shows the cross-sectional structures of various parts of a dactylopodite. The thickness ratios between the exocuticle and the endocuticle differed among cross sections with different diameters. Figure 4a shows a cross section of the first section of the specimen shown in Figure 2. The thicknesses of the exocuticle and endocuticle were 382.4 and 304.6 μm , respectively, yielding a ratio of 1.26. Figure 4b shows a cross section of the third section of the specimen in Figure 2, in which the thicknesses of the exocuticle and endocuticle were 310.4 and 383.5 μm , respectively. The diameter of the third section of the sample was smaller than that of the first section, and the thickness ratio between the layers was 0.81. When the cross-sectional diameter was reduced, the thickness ratios between the exocuticle and the endocuticle were correspondingly reduced.

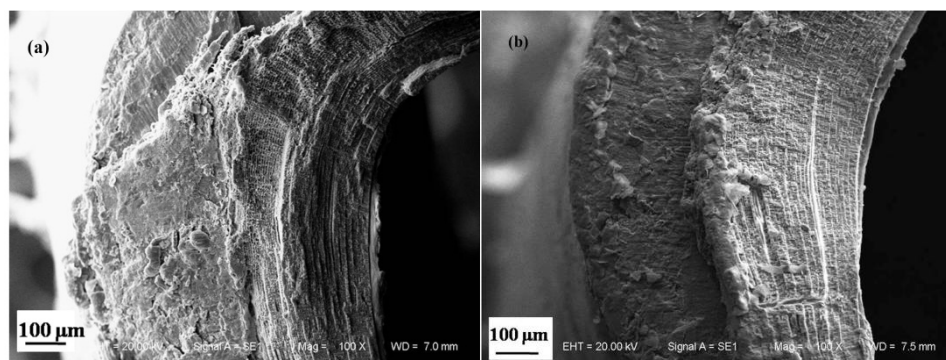


Figure 4. Thickness of the exocuticle and endocuticle at different positions along a Chinese mitten crab dactylopodite: (a) Section at $l = 5$ mm, (b) Section at $l = 15$ mm.

For the same cross section, the thickness of the exocuticle and endocuticle changed with the concave–convex variation of the dactylopodite. Figures 3 and 4a show the microstructure of a cross section at $l = 5$ mm. The concave and convex areas are marked A and B, respectively, in Figure 5. The thickness of the exocuticle at position A was $140.7 \mu\text{m}$, which was only 36.79% of the exocuticle thickness at position B. That is, the structural profile was uneven within a single section of dactylopodite.

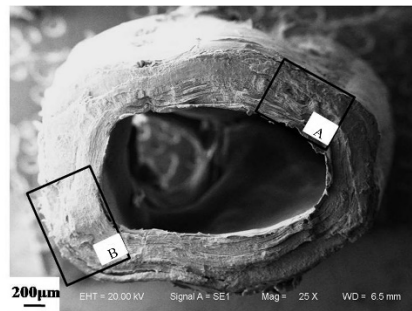


Figure 5. Concave (A) and convex (B) areas of the dactylopodite seen in cross section.

Figure 6 shows the layered structure of the cross section of the dactylopodite. The SEM results show no obvious stratified structure in the exocuticle layer (Figure 6a); however, a stratified structure was clear from the outside to the inside of the endocuticle layer, as shown in Figure 6b.

It can be seen in Figure 6c that the endocuticle is overlapped by multiple layers of fibers that are bounded by amorphous calcium bodies. The thickness of the fiber layer was about $6 \mu\text{m}$, and the thickness of the interlayer was about $1 \mu\text{m}$, forming a very dense, twisted, plywood-like structure known as a Bouligand structure [16]. Each layer contains an array of independent fiber bundles. The enlarged image shows that the fiber bundles in the same fiber layer are aligned along the same angle, which causes the fiber layer to intersect with the adjacent layers. Each group of fiber bundles consists of many filamentous fibers with a helical twist structure, as shown in Figure 6d. The cross section of the fiber bundle reveals tiny pores between fibers, as shown in Figure 6e. Interestingly, some fibers are interwoven in an orderly manner into crisscrossed crossing frames (Figure 6f), which increases the structure's toughness, stability, and strength.

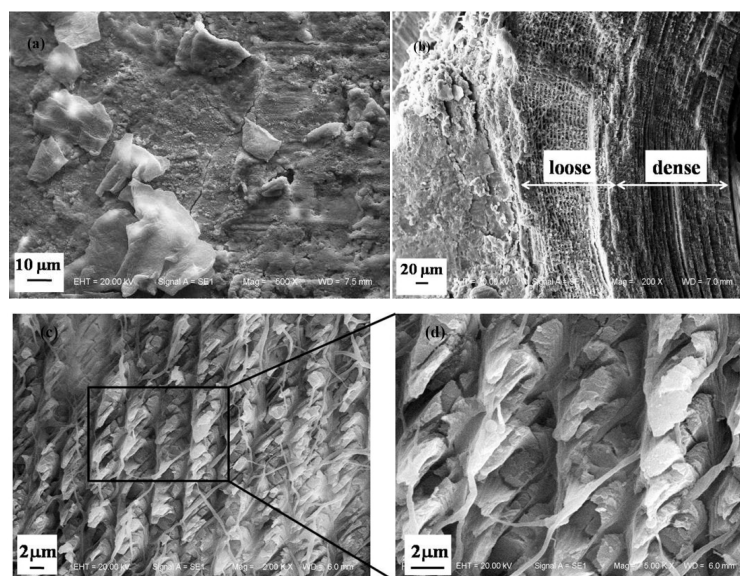


Figure 6. Cont.

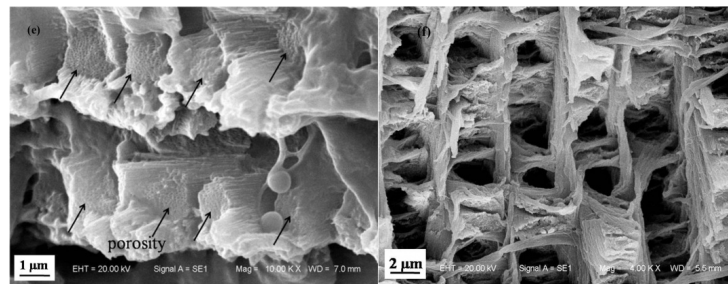


Figure 6. Layered microstructure of crosssections of Chinese mitten crab dactylopodite: (a) Exocuticle of dactylopodite, (b) endocuticle of dactylopodite, (c) Bouligand structure of endocuticle, (d) twisted filaments of fiber, (e) porosities between the fibers, (f) crossing frames.

3.1.2. Microstructure of Longitudinal Section of Dactylopodite

The SEM results show that the longitudinal sections of dactylopodites also had a layered structure (Figure 7). The fibrous layers of the endocuticle are densely arranged (Figure 8a), and its surface is densely covered with elliptic pore canals. The pore canals are formed by the crossing of fiber bundles (A in Figure 8b), with a helical band in each pore canal. The spiral ribbon (B in Figure 8b) is a pore canal tubule; these small tubes can transport nutrients across the exocuticle to new exoskeletons [17]. Meanwhile, soft and continuous tissues help increase the toughness of the exoskeleton. This porous structure can be observed in the fiber layers of many crustaceans, including the edible crab (*Cancer pagurus*) [18], the green crab (*Carcinus maenas*) [19], the American lobster (*Homarus americanus*) [20], and *Scapharca subcrenata* [21].

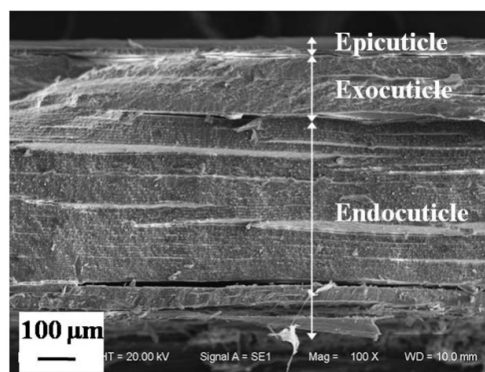


Figure 7. Layered structure in longitudinal section of dactylopodite.

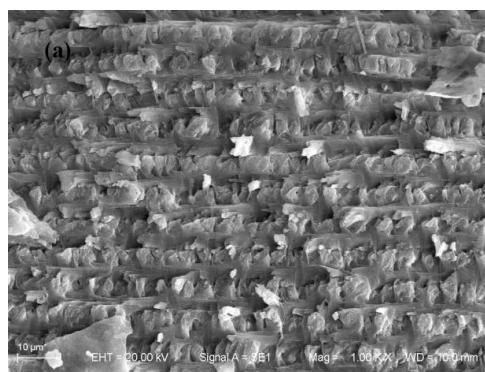


Figure 8. Cont.

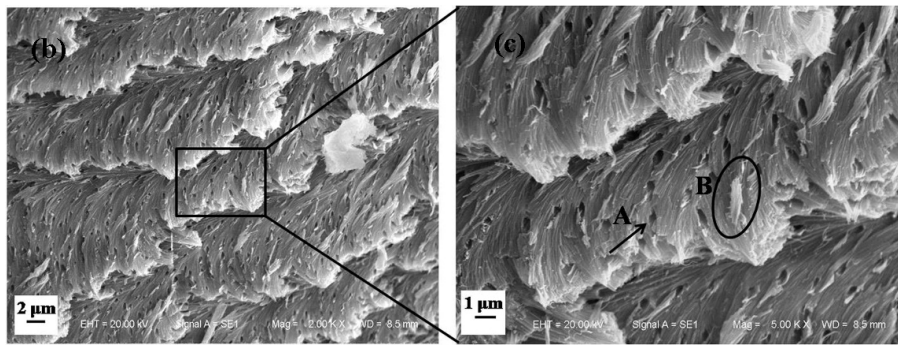


Figure 8. Microstructure of longitudinal section of dactylopodite: (a) Layered structure in exocuticle, (b,c) pore canal and pore canal tubule.

The tip of the dactylopodite is the part that makes the most frequent contact with the ground, rubbing and colliding with sand and gravel. It possesses high strength and abrasion resistance. As shown in Figure 9a, unlike the structure of the other parts of the dactylopodite, the exocuticle accounts for most of the exoskeleton at the tip, with a thickness about three times that of the endocuticle. The exocuticle at the tip is highly condensed, with pore channels crossing through it (Figure 9b). The endocuticle structure is similar to that in the other parts of the dactylopodites, with a Bouligand structure, as shown in Figure 9c. This kind of structure has high strength but maintains sufficient toughness to prevent the dactylopodites from being fractured by shock [16].

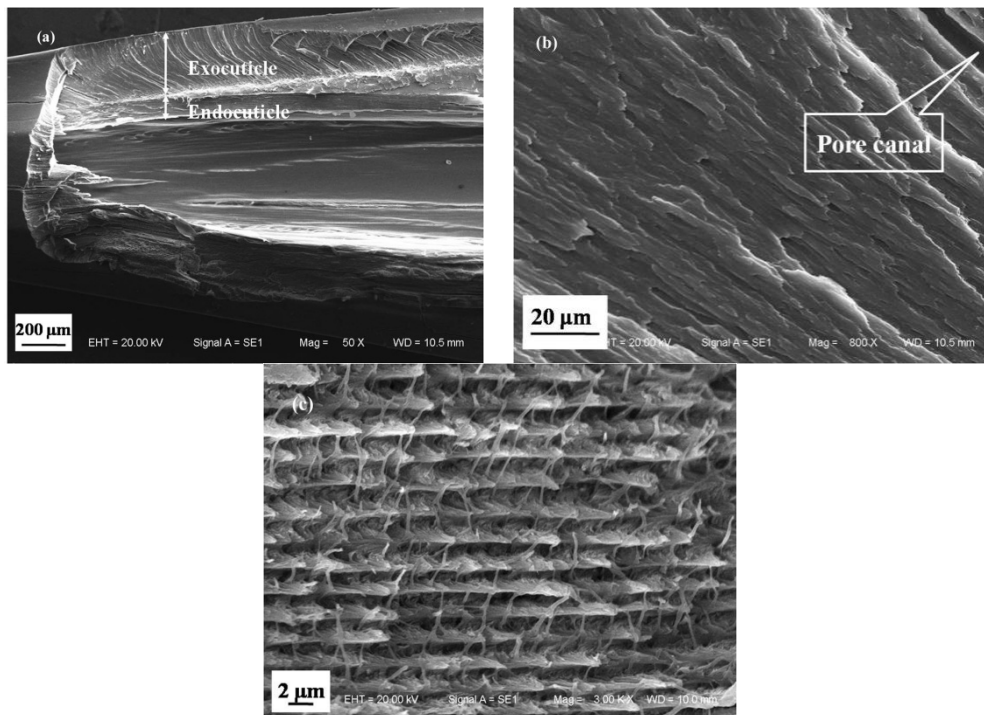


Figure 9. Longitudinal section of the tip of Chinese mitten crab dactylopodite: (a) Layered structure at tip of dactylopodite, (b) highly condensed structure of exocuticle, (c) Bouligand structure in endocuticle.

3.2. Material Properties

XRD and FTIR were used to analyze the material composition of the exoskeleton of the dactylopodites. The results of XRD analysis show a narrow band peak at $2\theta = 29.5^\circ$ with a full width at the half maximum (FWHM) of 0.27 and peak intensity of 180, indicating a crystalline structure.

In addition, smaller diffraction peaks were seen at $2\theta = 36.1^\circ$, 36.6° , 39.6° , 39.7° , 43.3° , and 48.8° , as shown in Figure 10. Comparative analysis [22] revealed that calcite is the predominant form of CaCO_3 in the exoskeleton.

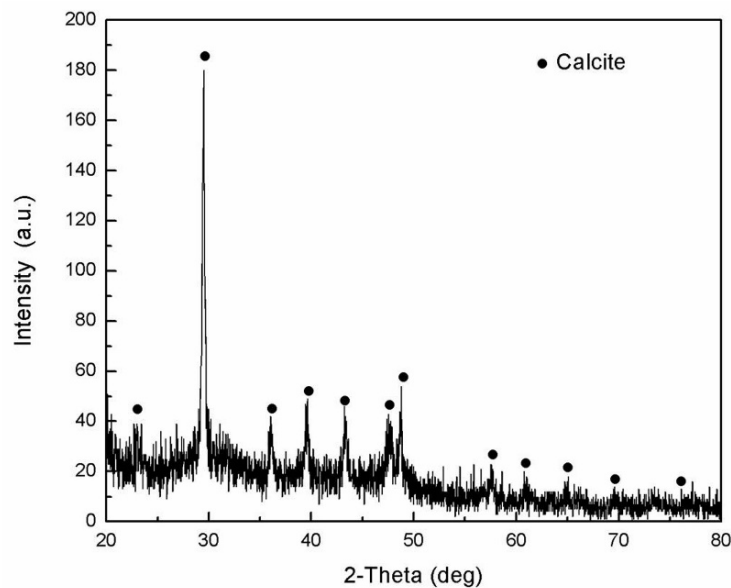


Figure 10. Results of XRD analysis.

Studies have shown that chitin is a common substance in the exoskeleton of crustaceans [23,24]. Kaya et al. [25] used FTIR analysis of the exoskeleton of the blue crab (*Callinectes sapidus*) and found O–H stretching at wave number 3432 cm^{-1} , CH_3 and CH_2 stretching at 2919 cm^{-1} , C=O secondary amide stretching at 1657 cm^{-1} , N–H bending and C–N stretching at 1550 cm^{-1} , C–O–C stretching at 1064 cm^{-1} , and C–H ring stretching at 890 cm^{-1} . The FTIR results for the grooved tiger prawn (*Penaeus semisulcatus*) showed that the same functional groups appeared at wave numbers 3438, 2918, 1656, 1562, 1072, and 899 cm^{-1} , respectively [26]. In the exoskeleton components of *Gammarus argaeus*, absorption peaks were shown at 3433, 2913, 1655, 1554, 1064, and 894 cm^{-1} [27], showing characteristics of the same functional groups.

Figure 11 shows the FTIR results of the Chinese mitten crab dactylopodite. The graph shows absorption peaks at 3440, 1635, 1408, 1075, 870, and 560 cm^{-1} . Compared with the results above, it can be concluded that the absorption peak of 3440 cm^{-1} is O–H stretching, 1635 cm^{-1} is C=O secondary amide stretching, 1408 cm^{-1} is N–H bend and C–N stretching, 1075 cm^{-1} is C–O stretching in the phase ring, and 870 cm^{-1} is closer to CH ring stretching. At 2930 cm^{-1} , weak CH_3 stretching and CH_2 stretching are seen.

The above analysis suggests that the organic components of the exoskeleton of the dactylopodites of the Chinese mitten crab are mainly chitin and protein fiber and that the inorganic component is mainly CaCO_3 in the form of crystallized calcite.

3.3. Mechanical Properties

Figure 12 illustrates the stress condition of hitting the ground and the supporting state when the Chinese mitten crab is moving, ignoring the force of friction and considering only the effect of the support reaction. Figure 12a shows the state when the tip of dactylopodite (T) comes into contact with the ground, and Figure 12b shows the state of the footstep during the supporting phase. When the dactylopodites are in contact with the ground and supporting, a bending moment will form at the end of the dactylopodite O' , due to the impulsive force and the support reaction F_N . If the bending

strength of the dactylopodite is insufficient, a bending fracture will occur. To observe the mechanical properties of dactylopodites, three-point bending tests were conducted on dry and wet specimens.

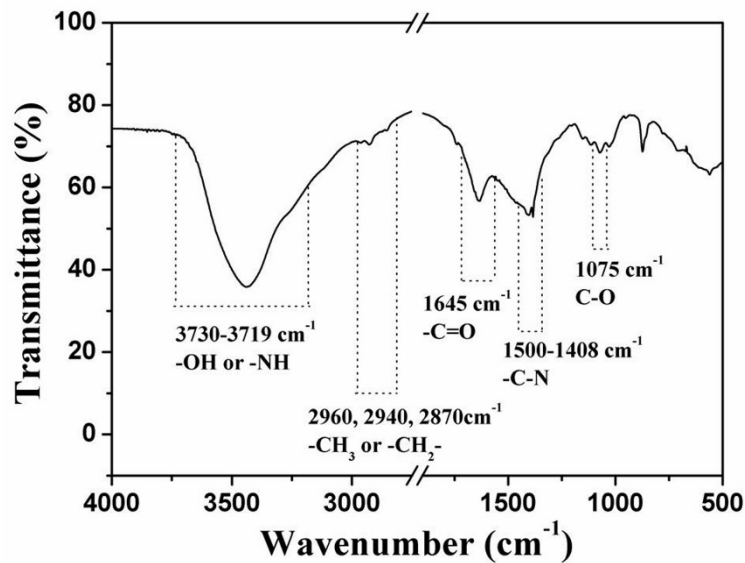


Figure 11. FTIR results for the dactylopodite exoskeleton.

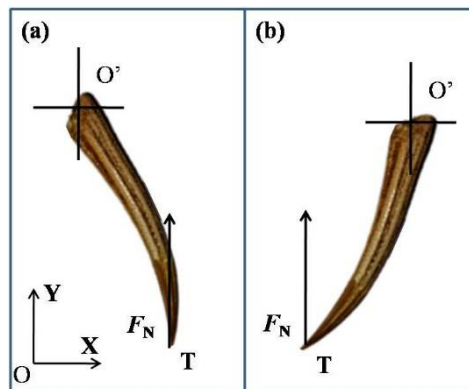


Figure 12. Forces on a dactylopodite during locomotion. (a) hitting the ground; (b) the supporting state.

The specimens for the three-point bending test were the second and third pairs of dactylopodites, which were divided into dry and wet samples. Table 2 shows the parameters of the samples. The tests were carried out by an in situ tensile tester. Each sample was fixed on the holders, and the span was 15 mm. Then load on it with pressure head driven by a motor at a constant speed until the samples were broken.

Table 2. Parameters of dactylopodite samples used for three-point bending tests.

Samples	Parameters			
	Moisture Content ϕ (%)	Max. Outer Diameter D (mm)	Inner Diameter D (mm)	Length l (mm)
Dry	0	2.71 ± 0.28	1.39 ± 0.046	32.62 ± 1.95
Wet	41.06 ± 4.64	2.50 ± 0.15	1.31 ± 0.005	30.88 ± 1.16

The bending strength of a dactylopodite, which can be calculated by Equation (1), is affected by a number of factors, including the structure, composition, and size. The cross section of the Chinese mitten crab dactylopodite is irregularly oblong with curved grooves on its circumference and has a variable cross section arc structure. Its composition is nonhomogeneous. The section modulus of the bending section is difficult to calculate accurately. Therefore the cross section of dactylopodite was approximated as annular in calculation. Thus M is proportional to load F and span L , and the module of bending section is anti-correlated with the third power of diameter of section D approximately. The bending stress can be calculated accordingly:

$$\sigma_b = \frac{M}{W} = \frac{FL/4}{\pi D^3(1 - \alpha^4)/32} \quad (1)$$

where M is the bending moment, W is the module of bending section, F is the load applied, L is span, α indicates d/D , $\pi(1 - \alpha^4)/32 \approx 0.092$.

Figure 13 shows a set of curves for bending stress–displacement. The bending stress of the dry specimens increases linearly with the displacement of indenter, reaches a maximum value of 56.781 MPa, then drops rapidly and decreases at about 0.553 mm. The bending load of the wet specimen increases with displacement and reaches a maximum of 85.525 MPa at 0.780 mm, then begins to decrease slowly and drops dramatically at 1.357 mm. The results show that the dry dactylopodites exhibited typical characteristics of brittle material, and the change of the bending stress curve was linear and tended to break within a small displacement. The wet specimens were distorted when loaded during the test, so the maximum bending stress occurred after a longer displacement. The slow decrease of the bending stress in the later period of the test also showed that as the indenter displacement increased, even though the tensile stress on the back of the dactylopodite increased and the specimen deformed to a large degree, it did not break, indicating the strength of the wet dactylopodite.

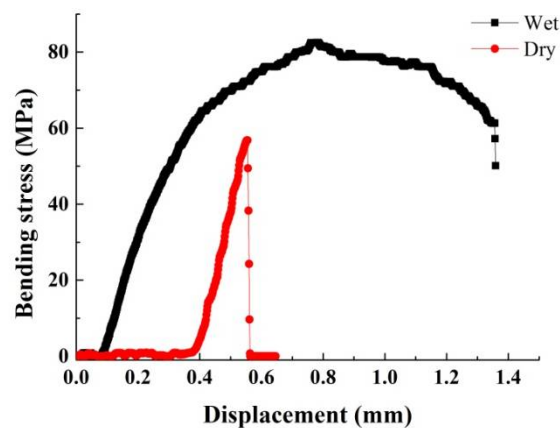


Figure 13. Curves of bending stress–displacement.

Figure 14 shows the statistics of the maximum value of bending stress and the corresponding displacement of indenter moved. Comparing the average maximum of dry and wet samples, the maximum bending stress they were able to withstand were about 63.339 ± 9.483 MPa and 81.817 ± 15.884 MPa, respectively, which indicated an excellent mechanical property of Chinese mitten crab dactylopodite. The bending stress of the wet samples was 29.17% higher than that of the dry samples. The displacement of indenter reflects the deformation of samples, which indicates they have better toughness with greater deformation under the higher load. In the figure, the average displacements for dry and wet samples are approximately 0.594 ± 0.044 mm and 0.698 ± 0.078 mm, respectively, at the time of stress reaching the maximum. It is well known that biomechanical properties depend greatly on hydration [28]. The results of the three-point bending experiment show

that moisture content influenced the bending strength of the dactylopodites and that the failure stress as greater for the wet dactylopodites than for the dry ones, which is consistent with the results conducted by Hepburn et al. on wet and dry specimens of mud crab (*Scylla serrata*) [29].

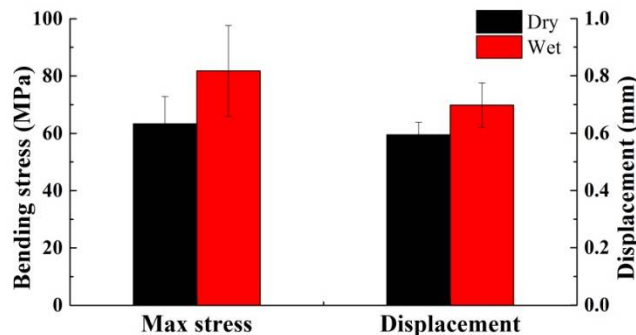


Figure 14. Comparison of stress and displacement for dry and wet samples.

4. Conclusions

In this work, the structure and mechanical properties of the dactylopodites of Chinese mitten crab were investigated. The conclusions are as follows.

1. The exoskeleton of the dactylopodites of Chinese mitten crab is multilayered, with an epicuticle, exocuticle and endocuticle. The thickness ratio of each layer is related to the section diameter and the concave and convex aspects of the profile. As the cross-sectional diameter decreases, the thicknesses of the exocuticle and endocuticle reduce and increase, respectively. For a given section, the thickness of the concave area is less than that of the convex area.
2. Cross sections and longitudinal sections of the endocuticle of the exoskeleton of the dactylopodites reveal a Bouligand structure, which benefits their mechanical properties. Each layer of the fibrous layer consists of several regularly arranged fiber bundles. Many pore canals are distributed regularly in the fiber layer, in which pore canal tubules transport nutrients while increasing the toughness of the inner epidermis.
3. The main organic constituents of the exoskeleton of the dactylopodites are chitin and protein, and the major inorganic compound is CaCO_3 crystallized as calcite.
4. Due to their structure and composition, the dry dactylopodites had characteristics of brittle materials, whereas the wet dactylopodites had characteristics of ductile materials.

Author Contributions: Xiujuan Li and Jianqiao Li conceived and designed the initial idea; Xiujuan Li analyzed and interpreted experiments data; Ying Wang wrote the article manuscript; Feng Qiu revised the manuscript for publication.

Funding: This research received no external funding.

Acknowledgments: This work was supported by the National Natural Science Foundation of China (No. U1601203) and Postdoctoral Science Foundation of China (No. 801161050414).

Conflicts of Interest: The authors declare no conflict of interest.

References

1. Wang, G.B.; Chen, D.S.; Chen, K.W.; Zhang, Z.Q. The current research status and development strategy on biomimetic robot. *J. Mech. Eng.* **2015**, *51*, 27–44. [[CrossRef](#)]
2. Zhuang, H.C.; Gao, H.B.; Deng, Z.Q. Analysis method of articulated torque of heavy-duty six-legged robot under its quadrangular gait. *Appl. Sci.* **2016**, *6*, 323. [[CrossRef](#)]
3. Yang, W.X.; Zhou, H. Primary study on the histology of exoskeleton of female pleopod in *Eriocheir sinensis*. *Dong Hai Mar. Sci.* **2000**, *9*, 29–33.

4. Neville, A.C. *Biology of the Arthropod Cuticle*; Springer: New York, NY, USA, 1975.
5. Vincent, J.F. *Structural Biomaterials*; Princeton University Press: Princeton, NJ, USA, 1991.
6. Vincent, J.F. Arthropod cuticle: A natural composite shell system. *Composites A* **2002**, *33*, 1311–1315. [[CrossRef](#)]
7. Herborg, L.M.; Rushton, S.P.; Clare, A.S.; Bentley, M.G. Spread of the Chinese mitten crab (*Eriocheir sinensis* H. Milne Edwards) in Continental Europe: Analysis of a historical data set. *Hydrobiologia* **2003**, *503*, 21–28. [[CrossRef](#)]
8. Clark, P.F.; Rainbow, P.S.; Robbins, R.S. The alien Chinese mitten crab, *Eriocheir sinensis* (Crustacea: Decapoda: Brachyura), in the Thames catchment. *J. Mar. Biol. Assoc. UK* **1998**, *78*, 1215–1221. [[CrossRef](#)]
9. Li, J.Q.; Zhang, X.D.; Zou, M.; Zhang, R.; Chirende, B.; Shi, R.Y.; Wei, C.G. An experimental study on the gait patterns and kinematics of Chinese mitten crabs. *J. Bionic Eng.* **2013**, *10*, 305–315. [[CrossRef](#)]
10. Zhang, X.D.; Li, J.Q.; Zou, M.; Zhang, R.; Li, Y.W. Three-dimensional observation and dynamics analysis of Chinese mitten crab's locomotion on smooth terrain. *Trans. Chin. Soc. Agric. Eng.* **2013**, *29*, 30–37.
11. Li, J.Q.; Zhang, X.D.; Zou, M.; Li, H.; Wang, Y.; Shi, R.Y. 3-D surveying and gait analysis of Chinese mitten crab in smooth road. *Trans. Chin. Soc. Agric. Eng.* **2012**, *43*, 335–338.
12. Wang, G.; Zhang, L.X.; Wang, L.Q. Research on a gait planning method for a crab-like octopod robot. *J. Harbin Eng. Univ.* **2011**, *32*, 486–491.
13. Wang, Y.; Li, J.Q.; Li, X.J.; Huang, H.; Qiu, F. Bionic Walking Foot and Mechanical Performance on Soil. *Appl. Sci.* **2017**, *7*, 575. [[CrossRef](#)]
14. Elices, M. *Structural Biological Materials: Design and Structure-Property Relationships*; Pergamon: Elmsford, NY, USA, 2000.
15. Raabe, D.; Romano, P.; Sachs, C.; Fabritius, H.; Sawalmih, A.; Yi, S.B.; Servos, G.; Hartwig, H.G. Microstructure and crystallographic texture of the chitin-protein network in the biological composite material of the exoskeleton of the lobster *Homarus americanus*. *Mater. Sci. Eng. A* **2006**, *421*, 143–153. [[CrossRef](#)]
16. James, C.; Weaver, G.W.; Milliron, A.M.; Kenneth, E.L.; Steven, H.I.; William, J.M.; Brook, S.P.; Zavattieri, E.D.; David, K. The Stomatopod Dactyl Club: A Formidable Damage-Tolerant Biological Hammer. *Science* **2012**, *336*, 8.
17. Compere, P.; Goffinet, G. Elaboration and ultrastructural changes in the pore canal system of the mineralized cuticle of *Carcinus maenas* during the molting cycle. *Tissue Cell* **1987**, *19*, 859–875. [[CrossRef](#)]
18. Hegdahl, T.; Silness, J.; Gustavsen, F. The structure and mineralization of the carapace of the crab (*Cancer pagurus* L)—1. The endocuticle. *Zool. Scr.* **1977**, *6*, 89–99.
19. Roer, R.D. Mechanisms of resorption and deposition of calcium in the carapace of the crab *Carcinus maenas*. *J. Exp. Biol.* **1980**, *88*, 205–218.
20. Sawalmih, A.; Li, C.; Siegel, S.; Fabritius, H.; Yi, S.; Raabe, D.; Fratzl, P.; Paris, O. Microtexture and chitin/calcite orientation relationship in the mineralized exoskeleton of the American lobster. *Adv. Funct. Mater.* **2008**, *18*, 3307–3314. [[CrossRef](#)]
21. Tian, X.M.; Han, Z.W.; Li, X.J.; Pu, Z.G.; Ren, L.Q. Biological coupling anti-wear properties of three typical molluscan shells *Scapharca subcrenata*, *Rapana venosa* and *Acanthochiton rubrolineatus*. *Sci. China Technol. Sci.* **2010**, *53*, 2905–2913. [[CrossRef](#)]
22. Liang, Y.H.; Zhao, Q.; Li, X.J.; Zhang, Z.H.; Ren, L.Q. Study of the microstructure and mechanical properties of white clam shell. *Micron* **2016**, *87*, 10–17. [[CrossRef](#)] [[PubMed](#)]
23. Kaya, M.; Karaarslan, M.; Baran, T.; Can, E.; Ekemen, G.; Bitim, B.; Duman, F. The quick extraction of chitin from an epizoic crustacean species (*Chelonibia patula*). *Nat. Prod. Res.* **2014**, *28*, 2186–2190. [[CrossRef](#)] [[PubMed](#)]
24. Bolat, Y.; Bilgin, S.; Günlü, A.; İzci, L.; Bahadır, K.S.; Çetinkaya, S. Chitin-chitosan yield of freshwater crab (*Potamon potamios*, Olivier 1804) shell. *Pak. Vet. J.* **2010**, *30*, 227–231.
25. Kaya, M.; Dudaklı, F.; Asan, O.M.; Cakmak, Y.S.; Baran, T.; Menten, A.; Erdogan, S. Porous and nanofiber a-chitosan obtained from blue crab (*Callinectes sapidus*) tested for antimicrobial and antioxidant activities. *LWT-Food Sci. Technol.* **2016**, *65*, 1109–1117. [[CrossRef](#)]
26. Sagheer, F.A.; Sughayer, M.A.; Muslim, S.; Elsabee, M.Z. Extraction and characterization of chitin and chitosan from marine sources in Arabian Gulf. *Carbohydr. Polym.* **2009**, *77*, 410–419. [[CrossRef](#)]

27. Kaya, M.; Tozak, K.O.; Baran, T.; Sezen, G.; Sargin, I. Natural porous and nano fiber chitin structure from *Gammarus argaeus* (*Gammaridae Crustacea*). *EXCLI J.* **2013**, *12*, 503–510. [[PubMed](#)]
28. Jiao, D.; Liu, Z.Q.; Qu, R.T.; Zhang, Z.F. Anisotropic mechanical behaviors and their structural dependences of crossed-lamellar structure in a bivalve shell. *Mater. Sci. Eng. C* **2016**, *59*, 828–837. [[CrossRef](#)] [[PubMed](#)]
29. Hepburn, H.R.; Joffe, I.; Green, N.; Nelson, K.J. Mechanical properties of a crab shell. *Comp. Biochem. Physiol.* **1975**, *50*, 551–554. [[CrossRef](#)]



© 2018 by the authors. Licensee MDPI, Basel, Switzerland. This article is an open access article distributed under the terms and conditions of the Creative Commons Attribution (CC BY) license (<http://creativecommons.org/licenses/by/4.0/>).